LJMU Research Online

Dybek, M, Wallach, J, Kavanagh, PV, Colestock, T, Filbman, N, Dowling, G, Westphal, F, Elliott, SP, Adejare, A and Brandt, SD

Syntheses and analytical characterizations of the research chemical 1-[1-(2-fluorophenyl)-2-phenylethyl]pyrrolidine (fluorolintane) and five of its isomers

http://researchonline.ljmu.ac.uk/id/eprint/10591/

Article

http://researchonline.ljmu.ac.uk/

Syntheses and analytical characterizations of the research chemical 1-[1-(2-fluorophenyl)-2-phenylethyl]pyrrolidine (fluorolintane) and five of its isomers

Michael Dybek,[a] Jason Wallach,[a] Pierce V. Kavanagh,[b] Tristan Colestock, [a] Nadine Filbman,[a] Geraldine Dowling,[b,c] Folker Westphal,[d] Simon P. Elliott,[e] Adeboye Adejare,[a] Simon D. Brandt [f,*]

[a] Department of Pharmaceutical Sciences, University of the Sciences, 600 South 43rd Street, Philadelphia, PA 19104, USA

[b] Department of Pharmacology and Therapeutics, School of Medicine, Trinity Centre for Health Sciences, St. James's Hospital, James's Street, Dublin 8, D08W9RT, Ireland

[c] Department of Life Sciences, School of Science, Sligo Institute of Technology, Ash Lane, Sligo, F91YW50, Ireland

[d] State Bureau of Criminal Investigation Schleswig-Holstein, Section Narcotics/Toxicology, Mühlenweg 166, D-24116 Kiel, Germany

[e] Elliott Forensic Consulting, Birmingham, UK

[f] School of Pharmacy and Biomolecular Sciences, Liverpool John Moores University, Byrom Street, Liverpool, L3 3AF, UK

*Corresponding author: Simon D. Brandt, School of Pharmacy and Biomolecular Sciences, Liverpool John Moores University, Byrom Street, Liverpool, L3 3AF, UK. E-Mail: s.brandt@ljmu.ac.uk

Running title: Characterizations of racemic fluorolintane isomers

Abstract

A number of substances based on the 1,2-diarylethylamine template have been investigated for various potential clinical applications whereas others have been encountered as research chemicals sold for non-medical use. Some of these substances have transpired to function as NMDA receptor antagonists that elicit dissociative effects in people who use these substances recreationally. 1-[1-(2-Fluorophenyl)-2-phenylethyl]pyrrolidine (fluorolintane, 2-F-DPPy) has recently appeared as a research chemical, which users report has dissociative effects. One common difficulty encountered by stakeholders confronting the appearance of new psychoactive substances is the presence of positional isomers. In the case of fluorolintane, the presence of the fluorine substituent on either the phenyl and benzyl moieties of the 1,2-diarylethylamine structure results in a total number of six possible racemic isomers, namely 2-F-, 3-F-, and 4-F-DPPy (phenyl ring substituents) and 2''-F-, 3''-F-, and 4''-F-DPPy (benzyl ring substituents). The present study reports the chemical syntheses and comprehensive analytical characterizations of the two sets of three positional isomers. These studies included various low- and high-resolution mass spectrometry platforms, gas- and liquid chromatography (GC and LC), nuclear magnetic resonance spectroscopy (NMR) and GC-condensed phase and attenuated total reflection infrared spectroscopy analyses. The differentiation between each set of three isomers was possible under a variety of experimental conditions including GC chemical ionization triple quadrupole tandem mass spectrometric analysis of the $[M + H - HF]^+$ species. The latter MS method was particularly helpful as it revealed distinct formation of product ions for each of the six investigated substances.

1. Introduction

The 1,2-diarylethylamine template gives rise to a range of substances that have been evaluated for various properties including neuroprotective, anticonvulsant, analgesic, bronchodilator and sympathomimetic effects.[1-3] More recent examples include remacemide and lanicemine that have undergone clinical investigations in areas linked to depression, seizure, stroke, and neurodegenerative disorders.[4,5] At the same time, a number of 1,2-diphenylethylamines, including diphenidine and methoxyphenidine, have attracted attention due to their appearance and classification as new psychoactive substances (NPS) and reports of non-medical use.[6] A common pharmacological feature shared between many 1,2-diarylethylamines and related arylcyclohexylamines including phencyclidine (PCP) and ketamine (Figure 1) is NMDA receptor blockage and dissociative effects in humans.[6-8] 1-[1-(2-Fluorophenyl)-2-phenylethyl]pyrrolidine (fluorolintane, 2-FPPP, 2-F-DPPy) (Figure 1) has appeared as a research chemical and is reported to display dissociative properties in users[7] though its pharmacological and analytical properties have not yet been extensively characterized. Fluorolintane is also the fluorinated derivative of 1-(1,2-diphenylethyl)pyrrolidine or DPPy, which has been investigated as an NMDAR antagonist for possible neuroprotective activities.[9] The nomenclature DPPy for 1-(1,2-diphenylethyl)pyrrolidine was chosen to be consistent with the arylcycloalkylamine nomenclature used given the overlapping benzylamine

2

pharmacophore of these two series. Thus the first two letters (DP) refer to the diphenyl rings and the last two letters (Py) refers to the pyrrolidine ring. Similarly diphenidine is abbreviated DPP.[7]

Following on from previous work on the analytical and pharmacological characterization of dissociative substances,[10-15] it was considered necessary to extend the explorations to emerging NPS of this type. Some basic analytical data for fluorolintane are available in the public domain[16] and a synthetic route has recently been described.[17] The enantioselective preparations of 2''-F-DPPy and 4''-F-DPPy (Figure 1) by hydrogenation of the enamine precursor have also been reported.[18,19] However, more extensive characterizations are currently unavailable. Whilst fluorolintane is available commercially from chemical suppliers, a frequent challenge in the detection of emerging NPS includes the differentiation between positional isomers. In the case of fluorolintane (2-F-DPPy), the fluorine substituent is located at the 2-position of the phenyl ring, which means that five additional racemic isomers are possible if one considers the potential presence of the fluorine substituent at the phenyl or benzyl moiety, thus leading to six possible racemic isomers (Figure 1). The present study reports on the syntheses of these racemates followed by comprehensive analytical characterizations using various mass spectrometry (MS) platforms, gas- and liquid chromatography (GC and LC), nuclear magnetic resonance spectroscopy (NMR) and infrared (IR) analysis. It is aimed to make these analytical data available to those stakeholders who are confronted with newly emerging psychoactive substances. Pharmacological studies carried out by the authors revealed the substances' interaction with the N-methyl-D-aspartate (NMDA) receptor and other biological targets including monoamine transporters that will be reported elsewhere.

2. Experimental

2.1 Reagents and standards

All chemicals used for syntheses were obtained from Sigma Aldrich (St Louis, MO, USA). Column chromatography was performed using Merck silica gel grade 9385 (230-400 mesh, 60 Å). Melting points were determined using a Digimelt A160 SRS digital melting point apparatus (Stanford Research Systems, Sunnyvale, CA, USA) at a ramp rate of 2 °C/min.

2.2 Syntheses

Preparation of 1-(1,2-diphenylethyl)pyrrolidine) (DPPy)

A suspension of benzyl bromide (1.12 mL, 9.42 mmol), zinc dust (<10 μm, 0.616 g, 9.42 mmol) and trifluoroacetic acid (90 μL, 1.18 mmol) in 40 mL of dry tetrahydrofuran (THF) was prepared with the exclusion of moisture and stirred for 20 min under argon. Upon reaching room temperature both pyrrolidine (430 μL, 5.18 mmol) and benzaldehyde (480 μL, 4.71 mmol) were added in rapid succession and allowed to react over 24 h at ambient temperature. Upon completion (confirmed by GC-MS), the reaction mixture was poured into 400 mL of 1 M HCl solution and washed three times

with 75 mL of ethyl acetate. These organic portions were pooled and extracted three times with 1 M HCl and the HCl extractions were combined with aqueous phase. The combined aqueous phase was then basified with ammonium hydroxide (aqueous ammonium hydroxide can also be used as a base but caused more abundant precipitation of inorganic solids) and extracted three times with ethyl acetate (3 x 100 mL). The pooled organic phases were washed with brine (10 mL), dried with anhydrous Na_2SO_4 and then the solvent was removed under reduced pressure to yield 820 mg crude material as a yellow oil. This material was purified via flash column chromatography utilizing silica gel as the stationary phase, and a mobile phase of ethyl acetate and hexanes (1:4) containing 1% triethylamine (TEA) to yield pure DPPy as a colorless oil (863 mg, 3.43 mmol, 73.2% yield calculated based on benzaldehyde). The purified material was converted into the HCl salt by titrating the free base with concentrated HCl solution in acetone until the pH < 2. The solvent was then evaporated under a stream of warm air several times to yield crystalline material in the absence of excess acid or moisture. The solids were washed with diethyl ether (2 x 10 mL) in order to remove any color and any ether soluble impurities that may have formed during the salt formation process. After the washes with ether, the resulting crystals were dissolved in 15 mL of boiling acetone and 65 mL of diethyl ether added subsequently to crystallize the salt. The crystals yielded were collected by gravity filtration and washed with diethyl ether (2 x 30 mL), dried by gentle heating, and re-crystallized from acetone and diethyl ether (1:4) as described for a total of four times. The final solid material was then dried first in an oven (75 °C) followed by storage in a desiccator under vacuum to yield DPPy hydrochloride collected as a white crystalline powder (m.p. 216.0–217.0 °C, lit. 212 °C[20]). HR-ASAP-MS observed at m/z 252.1752 (theory [M + H]$^+$ $C_{18}H_{22}N^+$, m/z 252.1747, Δ = 1.98 ppm).

Preparation of 1-[1-(2-fluorophenyl)-2-phenylethyl]pyrrolidine (2-F-DPPy)

2-F-DPPy was prepared as described above using 2-fluorobenzaldehyde as the starting material to give pure 2-F-DPPy as a colorless oil (731 mg, 2.71 mmol, 67.3% yield). QTOF-MS m/z 270.16556 (theory [M + H]$^+$ $C_{18}H_{21}FN^+$, m/z 270.16525, Δ = 1.1 ppm). The HCl salt was obtained as collected as colorless needles (m.p. 231.8–232.5 °C).

Preparation of 1-[1-(3-fluorophenyl)-2-phenylethyl]pyrrolidine (3-F-DPPy)

3-F-DPPy was prepared as described above using 3-fluorobenzaldehyde as the starting material to give pure 3-F-DPPy as a colorless oil (747 mg, 2.77 mmol, 68.5% yield). QTOF-MS m/z 270.16576 (theory [M + H]$^+$ $C_{18}H_{21}FN^+$, m/z 270.16525, Δ = 1.9 ppm). The HCl salt was collected as a white crystalline powder (m.p. 231.8–232.5 °C).

Preparation of 1-[1-(4-fluorophenyl)-2-phenylethyl]pyrrolidine (4-F-DPPy)

4-F-DPPy was prepared as described above using 4-fluorobenzaldehyde as the starting material to give pure 4-F-DPPy as a colorless oil (452 mg, 1.68 mmol, 41.7% yield). QTOF-MS m/z 270.16598 (theory [M + H]$^+$ $C_{18}H_{21}FN^+$, m/z 270.16525, Δ = 2.7 ppm). The HCl salt was collected as colorless needles (m.p. 215.7–216.8 °C).

Preparation of 1-[2-(2-fluorophenyl)-1-phenylethyl]pyrrolidine (2"-F-DPPy)

2"-F-DPPy was prepared as described above using 2-fluorobenzyl bromide as the starting material to give pure 2"-F-DPPy as a colorless oil (950 mg, 3.58 mmol, 76.0% yield). QTOF-MS m/z 270.16593 (theory [M + H]$^+$ C$_{18}$H$_{21}$FN$^+$, m/z 270.16525, Δ = 2.5 ppm). The HCl salt was collected as a white crystalline powder (m.p. 195.7–197.0 °C)

Preparation of 1-[2-(3-fluorophenyl)-1-phenylethyl]pyrrolidine (3"-F-DPPy)

3"-F-DPPy was prepared as described above using 3-fluorobenzyl bromide as the starting material to give pure 3"-F-DPPy as a colorless oil (721 mg, 2.68 mmol, 56.8% yield). QTOF-MS m/z 270.16593 (theory [M + H]$^+$ C$_{18}$H$_{21}$FN$^+$, m/z 270.16525, Δ = 2.5 ppm). The HCl salt was collected as fluffy colorless needles (m.p. 215.4–216.5°C)

Preparation of 1-[2-(4-fluorophenyl)-1-phenylethyl]pyrrolidine (4"-F-DPPy)

4"-F-DPPy was prepared as described above using 4-fluorobenzyl bromide as the starting material to give pure 4"-F-DPPy as a colorless oil (1003 mg, 3.88 mmol, 79.0% yield). QTOF-MS m/z 270.16585 (theory [M + H]$^+$ C$_{18}$H$_{21}$FN$^+$, m/z 270.16525, Δ = 2.2 ppm). The HCl salt was collected as thick colorless chunky solids (m.p. 207.2–209.0°C).

2.3 Instrumentation

2.3.1 Gas chromatography mass spectrometry

For electron ionization mass spectrometry (EI-MS), a Finnigan TSQ 8000 Evo triple stage quadrupole mass spectrometer coupled to a gas chromatograph (Trace GC 1310, Thermo Electron, Dreieich, Germany) and for chemical ionization (CI) MS a Finnigan TSQ 7000 triple stage quadrupole mass spectrometer coupled to a gas chromatograph (Trace GC Ultra, Thermo Electron, Dreieich, Germany) was used. A Triplus RSH (Thermo Scientific for TSQ 8000 Evo) and a CTC CombiPAL (CTC Analytics, Zwingen, Switzerland for TSQ 7000) autosampler was employed for sample introduction. Mass spectra were recorded at 70 eV electron ionization energy. The ion source temperature was set at 175°C and the emission current was 50 µA (TSQ 8000 Evo) and 400 µA (TSQ 7000). For recording of EI-MS the scan time was 1 s spanning a scan range between m/z 29–m/z 600 and samples were injected in splitless mode.

For CI, the reagent gas was methane and the source pressure was 1.5 mTorr (0.2 Pa). The scan time was 0.5 s and the scan range was m/z 50–m/z 600 and samples were injected in splitless mode.

In the CI-MS/MS-product-ion-mode, the ionization energy was 70 eV with an emission current of 400 µA and a source temperature of 175°C. The scan time was 1 s and the scan range started at m/z 10 and ended about 10 mass units above the ion that was examined. The collision gas was argon. The collision energy was approximately 20 eV and the collision gas pressure was approximately 1.5 mTorr (0.2 Pa). The exact target-thickness was set using *n*-butylbenzene in EI-MS mode and adjusting intensity ratios m/z 92/91 to 0.2 and m/z 65/91 to 0.02 by variation of collision energy and collision gas pressure. This method ensured reproducibility of

the product ion mass spectra and the use of a product ion mass spectra library for the identification of the structures of the product ions.

Separation was achieved using a fused silica capillary DB-1 column (30 m × 0.25 mm, film thickness 0.25 µm). The temperature program consisted of an initial temperature of 80°C, held for 2 min, followed by a ramp to 280°C at 15 °C/min. The final temperature was held for 20 min. The injector temperature was 280°C (TSQ 8000) and 220°C (TSQ 7000), respectively. The transfer line temperature was set at 280 °C and the carrier gas was helium in constant flow mode at a flow rate of 1.0 mL/min. Approximately 2 mg were dissolved in 2 mL of deionized water, alkalized with a few drops of 5 % (w/v) NaOH solution and extracted with 2 mL diethyl ether. For analysis, 1 µL of the extract was injected into the GC-MS system. Retention indices are given as Kovats indices calculated from measurement of a *n*-alkane mixture analyzed with the above mentioned temperature program.

2.3.2 Gas chromatography solid-state infrared analysis

Samples were analyzed using a GC-solid phase-IR-system that consisted of an Agilent GC 7890B (Waldbronn, Germany) with probe sampler Agilent G4567A and a DiscovIR-GC™ (Spectra Analysis, Marlborough, MA, USA). The column eluent was cryogenically accumulated on a spirally rotating ZnSe disk cooled by liquid nitrogen. IR spectra were recorded through the IR-transparent ZnSe disk using a nitrogen-cooled MCT detector. GC parameters: injection in splitless mode with an injection port temperature set at 240°C and a DB-1 fused silica capillary column (30 m × 0.32 mm i.d., 0.25 µm film thickness). The carrier gas was helium with a flow rate of 2.5 mL/min and the oven temperature program was as follows: 80°C for 2 min, ramped to 290°C at 20 °C/min, and held at for 20 min. The transfer line was heated at 280°C. Infrared conditions: oven temperature, restrictor temperature, disc temperature, and Dewar cap temperatures were 280°C, 280°C, -40°C, and 35°C, respectively. The vacuum was 0.2 mTorr, disc speed 3 mm/s, spiral separation was 1 mm, wavelength resolution 4 cm^{-1} and IR range 650–4000 cm^{-1}. Acquisition time was 0.6 s/file with 64 scans/spectrum. Data were processed using GRAMS/AI Ver. 9.1 (Grams Spectroscopy Software Suite, Thermo Fisher Scientific, Dreieich, Germany) followed by implementation of the OMNIC Software, Ver. 7.4.127 (Thermo Electron Corporation, Dreieich, Germany).

2.3.3 Infrared spectroscopy

IR spectra were recorded on a Nicolet 380 FT-IR with a Smart Golden Gate Diamant ATR (Thermo Fisher Scientific). The wavelength resolution was 4 cm^{-1}. IR spectra were collected in a range of 600–4000 cm^{-1} with 16 scans per spectrum. The IR data were processed using OMNIC Software, Ver. 7.4.127 (Thermo Electron Corporation). IR spectra of the free bases were recorded as neat film after the following sample preparation procedure: For the generation of the free bases, a few milligrams of the hydrochloride salts were dissolved in deionized water, alkalized with a few drops of aqueous NaOH solution (5% w/w) and extracted with diethyl ether. The organic phase was concentrated to approximately 100 µL by a gentle airflow, aspired with a glass pipette and transferred directly to the ATR crystal yielding a film of the free base after final evaporation of diethyl ether.

2.3.4 High mass accuracy electrospray ionization mass spectrometry

Ultrahigh-performance liquid chromatography quadrupole time-of-flight single and tandem mass spectrometry (UHPLC-QTOF-MS/MS) data were obtained from an Agilent 6540 UHD Accurate-Mass QTOF LC-MS system coupled to an Agilent 1290 Infinity UHPLC system (Agilent, Cheshire, UK). Separation was achieved using an Agilent Zorbax Eclipse Plus C18 column (100 mm × 2.1 mm, 1.8 μm) (Agilent, Cheadle, UK). Mobile phases consisted of acetonitrile (1% formic acid) and 1% formic acid in water. The column temperature was set at 40°C (0.6 mL/min) and data were acquired for 5.5 min. The gradient was set at 5–70% acetonitrile over 3.5 min, then increased to 95% acetonitrile in 1 min and held for 0.5 min before returning to 5% acetonitrile in 0.5 min. QTOF-MS data were acquired in positive mode scanning from m/z 100–m/z 1000 with and without auto MS/MS fragmentation. Ionization was achieved with an Agilent JetStream electrospray source and infused internal reference masses. QTOF-MS parameters: gas temperature 325°C, drying gas 10 L/min and sheath gas temperature 400°C. Internal reference ions at m/z 121.05087 and m/z 922.00979 were used for calibration purposes.

2.3.5 High performance liquid chromatography diode array detection

HPLC-DAD analyses were carried out on an Agilent/Hewlett Packard (Little Island, Co. Cork, Ireland/Santa Clara, CA, USA) 1100 system (G1322A degasser, G1311A quaternary pump, G1313A autosampler and G1315A UV-visible diode array detector) using a Cosmosil πNAP column (4.6 mm x 150 mm, 5 μm) (Nacalai Tesque, Inc., Kyoto, Japan). The injection volume, flow rate and ambient room temperature were 10 μL, 1.0 mL/min and 22°C, respectively. Mobile phase A consisted of 0.05 M ammonium formate (pH 10) and mobile phase B was acetonitrile. The gradient elution program was as follows. 0–1 min 50% A, 1–17 min down to 40% A, 17–18 min 40% A, 18–19 min up to 50% A, and 19–24 min 50% A. The diode array detection window was set at 200 nm to 400 nm (step, 2 nm).

2.3.6 Nuclear magnetic resonance (NMR) spectroscopy

^{1}H (400 MHz) and ^{13}C NMR spectra (101 MHz) were obtained from the hydrochloride salts (or in some cases freebases) in anhydrous d_6-DMSO solutions (20 mg/mL) (>99.9% D, Sigma Aldrich) on a Bruker Ultrashield 400 plus spectrometer with a 5 mm BBO S1 (Z gradient plus) probe at ambient temperature. Internal chemical shift references were solvent (δ = 2.50 and 39.52 ppm for ^{1}H and ^{13}C spectra respectively). ^{19}F (376.5 MHz) NMR was run as described using trichlorofluoromethane (99%+, Aldrich) as internal reference (δ = 0.0 ppm). NMR assignments were made using chemical shift position, splitting, ^{13}C and ^{13}C PENDANT and hetero- and homo- 2-D experiments such as HMQC, HMBC and COSY to confirm all assignments. A background water concentration of solvent (determined as integration ratio relative to solvent shift) was also determined in order to check for water content within the final salts.

3. Results and discussion

Syntheses of the described 1,2-diarylethylamines were performed utilizing a convenient one-pot reaction referred to as the modified Mannich-Barbier reaction. This procedure was adapted from that employed by Le Gall et al. for the preparation of an assortment of arylakylamines.[21] It is a three-component reaction involving a commercially available benzyl bromide, an aldehyde and an amine in the presence of zinc dust activated with trifluoroacetic acid (TFA). Both solvents acetonitrile and tetrahydrofuran (THF) gave good yields. The reaction can tolerate a very large scope of substitutions on both the benzyl bromide, aldehyde and amine. The reactions generally utilize convenient low cost reagents to produce final compounds in moderate to excellent yields. This method was utilized previously to prepare other 1,2-diarylethylamines such as 2-MXP and 2-Cl-DPP [12,13] and a range of other diphenidine analogs.[22] Finally, during final preparation of HCl salts, it was noticed via NMR that these crystals can form solvate co-crystals with methanol, ethanol, and isopropanol to differing degrees which led to the decision to employ acetone as the recrystallization solvent.

3.1. Analytical features

3.1.1 Mass spectrometry, chromatography and infrared spectroscopy

The electron ionization (EI) mass spectra recorded for the two sets of three positional isomers are shown in Figure 2. As expected, each set of three isomers resulted in comparable mass spectra whereas significant differences could be found between the two sets of analogs substituted at the phenyl ring (2-F-, 3-F-, 4-F-DPPy) and those carrying the fluorine substituent at the benzyl moiety (2''-F-, 3''-F-, 4''-F-DPPy). In the former case, the two most abundant fragments were observed at m/z 178 (base peak), proposed to reflect α-cleavage and formation of an iminium ion and m/z 109 that presumably represented the fluorinated tropylium species. Proposed fragmentation pathways using 4-F-DPPy as a representative example are depicted in Figure 3A. Correspondingly, the EI mass spectra of 2''-F-, 3''-F-, and 4''-F-DPPy revealed the presence of m/z 160 and m/z 91 as a consequence of the fluorine substituent being located at the benzyl moiety instead (Figures 2 and 3B). From the perspective of EI-MS analysis, differentiation between the isomers was thus possible between the two groups that reflected the fluorine substituent at the two aromatic rings. In the cases of diphenidine and methoxyphenidine (Figure 1), the base peaks equivalent to the m/z 178 and/or m/z 160 ions detected here were recorded at m/z 174 and m/z 204, reflecting the presence of the benzyl-piperidine and methoxybenzyl-piperidine moieties.[11,12] Previous investigations on DPPy are thereby consistent with the nonfluorinated analogs of 2-F-, 3''-F-, and 4''-F-DPPy investigated in this study, which also gave rise to the base peak at m/z 160.[11] A complete separation of all isomers using gas chromatography (GC) was unsuccessful under the conditions used, which was consistent with observations made during the investigation of three structurally related positional fluorinated isomers of 1-cyclohexyl-4-(1,2-diphenylethyl)piperazine (MT-45).[23]

Implementation of GC chemical ionization mass spectrometry (CI-MS) confirmed the protonated molecules at m/z 270 and detection of adducts associated with the

reagent gas (methane) [M + 29]$^+$ (m/z 298) and [M + 41]$^+$ (m/z 310) of minor abundance. In single stage CI-MS mode, the protonated molecule experienced some fragmentation that resulted in the detection of additional ions including m/z 250 that was considered consistent with [M + H – HF]$^+$ (Figure 4). Albeit at relatively low abundance, the m/z 72 ion, proposed to represent a pyrrolidin-1-ium species, could serve diagnostic purposes regarding the identity of the amine moiety. Correspondingly, diphenidine and methoxyphenidine (Figure 1) gave rise to m/z 86[11,12] whereas DPPy also yielded the m/z 72 ion.[11] Figure 5A depicts a proposed fragmentation pathway using 4-F-DPPy as a representative example. Similar to what was observed under EI-MS conditions, both sets of isomers yielded distinctive base peaks at m/z 178 and m/z 160 when subjected to analysis by CI-MS, possibly as a consequence of losing either toluene (Figure 5A) or fluorinated toluene, respectively (Figure 5B).

The formation of [M + H – HF]$^+$ under CI-MS conditions at m/z 250 prompted further investigations by employing additional GC-CI-QqQ-MS/MS experiments, which was found to be particularly helpful as this enabled differentiation between all six isomers (Figure 6). 2-F-DPPy generated the most extensive number of product ions where abundant ions detections included m/z 70, 103, 131, 158, 159, 166, 179, and m/z 181 (base peak). Key ions recorded for 3-F-DPPy included m/z 91, 159, 174 (base peak), and m/z 179. In case of 4-F-DPPy, the [M + H – HF]$^+$ ion maintained highest stability (base peak) but less abundant ions were detected including m/z 91, 159, and m/z 181 (Figure 6). The CI tandem mass spectra collected for the second set of isomers substituted at the benzyl group differed both in all three cases but also from fluorolintane (2-F-DPPy) and its two fluorophenyl positional isomers. Interestingly, the [M + H – HF]$^+$ ion at m/z 250 remained most stable in the mass spectrum derived from 2''-F-DPPy whereas it was absent in the spectrum of 3''-F-DPPy, which was dominated by the base peak at m/z 160. In comparison, the base peak detected for 4''-F-DPPY was detected at m/z 158 together with a number of product ions of low to moderate abundance including m/z 130, 144, 166, 173, and m/z 181, respectively (Figure 6). The combination of using chemical ionization with tandem mass spectra analysis of the [M + H – HF]$^+$ ion has been previously reported to also facilitate the differentiation between various fluorinated amphetamine and cathinone isomers.[24,25] A suggested fragmentation scheme, using 2-F-DPPy and 4''-F-DPPY as representative examples, is presented in Figure 7.

UHPLC-ESI-QTOF-MS/MS analysis results are presented in Figure 8, which indicated that both chromatographic and mass spectrometric information were insufficient to facilitate a differentiation between the isomers. Main ions included m/z 72, 103, 121, 159, 179 and m/z 199 (base peak). Implementing the high mass accuracy option supported the formulation of proposed dissociation pathways suggested in Figure 9. The base peak at m/z 199 was thought to arise from loss of pyrrolidine from the protonated molecule. To some extent, this loss was also observable under CI-MS conditions although the abundance of m/z 199 was comparatively low to moderate in comparison. The equivalent species of m/z 199 reported for diphenidine, methoxdiphenidine, and DPPy following ESI-QqQ-MS/MS analysis were m/z 166, m/z 211, and m/z 166.[11,12] Similar to what was observed under CI-MS conditions, the detection of m/z 72 was diagnostic for the pyrrolidine component ($C_4H_{10}N^+$).

As far as HPLC-based analyses were concerned, initial attempts to achieve adequate separations with various standard C18 columns proved unsuccessful but then it was hypothesized that an increase in π-π interactions between column stationary phase and analytes (under alkaline conditions) might be beneficial. As depicted in Figure 10, adequate separations of isomers were obtained when employing a stationary phase containing naphthalene bonded silica packing material (Cosmosil πNAP column). However, the separation of all six isomers was not successful within the same chromatographic run. The implementation of a Hypersil GOLD™ PFP column was reported to facilitate the separation of three fluorinated amphetamine and methamphetamine isomers.[26] As expected, inspection of all UV full scan spectra recorded from HPLC-DAD analysis revealed that no specific differences between the six isomeric compounds could be identified (supporting information).

The implementation of GC condensed phase IR analysis (GC-sIR) allows for the collection of spectral data directly from chromatographic peaks whereby the analyte is deposited cryogenically onto an IR-transparent zinc selenide disk. The advantage of employing this method is that IR spectra are recorded in a solid state comparable to freebase spectra recorded under traditional conditions; for example, by using a Fourier transform attenuated total reflection (ATR) approach. Figures 11 and 12 show a partial section of the IR spectrum for the purpose of comparison. A direct comparison indicated that the three isomers within each group (2-F-, 3-F-, 4-F- and 2''-F-, 3''-F-, 4''-F-DPPy) yielded distinctive IR spectra. IR spectra collected over the full scan range (as HCl salts, freebase and GC-sIR) are provided as Supporting Information. For example, the IR spectra of 4-F-DPPy and 4''-F-DPPy contained sharp intense band at 1220 cm^{-1} and, in particular, at 1510 cm^{-1}, which distinguish this isomer form the two other isomeric sets. A comparison of 2-F/2''-F-, 3-F/3''-F-, and 4-F/4''-F-DPPy also indicated that differences identified in the IR spectra were still observable (Figures 11 and 12) (supporting information).

3.1.2 Nuclear magnetic resonance spectroscopy (NMR)

3.1.2.1 Aliphatic ^{1}H chemical shifts

The aliphatic ^{1}H spectra measured with the current series were consistent with those reported previously for diphenidine and several related 1,2-diarylethylamines (Tables 1 and 2).[11,12] In order to determine the effect of fluorine substitution on chemical shift behavior, DPPy was also evaluated. ^{1}H chemical shift assignments for the HCl salts of DPPy, fluorolintane and its 5 positional fluorine-isomers are presented in Tables 1 and 2. In addition, the freebase spectra and assignments for fluorolintane are provided as Supporting Information.

In all compounds, the assigned H_1 shift was always shifted downfield relative to H_2, with the latter giving separate multiplets (each integrating to 1 proton) for both protons. The substitution with fluorine in the phenyl-substituted series (i.e., 2-, 3-, 4-F series) in 2-F-DPPy, led to a further downfield shift of H_1 relative to DPPy, and compared to the corresponding $C_{1''}$ benzyl-substituted (i.e., 2''-, 3'-', 4''-F isomers). This shift was most dramatic in the case of 2-F-DPPy (~0.3 ppm) likely due to the

closer proximity of the fluorine substitution causing an inductive deshielding effect, followed by 3-F-DPPy with only a modest effect (0.05 ppm). Supporting this, no comparable fluorine effect on the H_2 ^1H chemical shift was observed with the phenyl-substituted series. A comparable effect was observed with 2''-F-DPPy (but not other benzyl series isomers), however in which one of the two ^1H chemical shifts assigned to H_2 (the more upfield shift) was shifted (0.13 ppm) downfield relative to DPPy. Again, the relative downfield shift for the H_2 ^1H chemical shift for 2''-F-DPPy, was likely the result of inductive deshielding effects. This downfield shift is thus potentially of analytical value for distinguishing the 2-F-DPPy and 2''-F-DPPy isomers using the ^1H spectra.

The ^1H chemical shifts assigned to H_α of the pyrrolidine ring appeared as up to four separate multiplets. Whereas four separate multiplets were observed in most cases, in a few cases (such as the upfield shifts of 2''-F and 4''-F), the upfield multiplet coalesced and the resulting broad multiplets integrated to two protons. The H_β ^1H chemical shifts were also complex and appeared either as a single broad multiplet as in 2-F-DPPy or in all other cases as three separate multiplets, in which the most downfield multiplet integrated to two protons.

It is worth noting that in the corresponding ^{13}C spectra, the C_α and C_β ^{13}C shifts appeared as two distinct ^{13}C chemical shifts, with each ^{13}C shift showing cross correlation with one or more ^1H multiplets (integrating for a total of 2 protons) in the HMQC spectra. In these 2-dimensional spectra, the upfield ^{13}C shift always correlated with the two most upfield proton shift(s) and vice versa for the downfield shifts.

These magnetic nonequivalence patterns for C_α and C_β shifts observed in the ^1H and ^{13}C spectra, are likely the result of amine nitrogen protonation inducing a distinct conformational state of the pyrrolidine ring, which led to asymmetry in the electronic environments experienced by the otherwise symmetric protons causing magnetic nonequivalence under the experimental conditions. This nonequivalence is supported by the fact that in the case of fluorolintane freebase (supporting information) the ^1H chemical shifts assigned to H_α appeared as two multiplets (integrating to two each and thus representing axial and equatorial protons) and the corresponding ^{13}C shifts for C_α and C_β each appeared as a single chemical shift. This phenomenon has been observed previously with diphenidine and related compounds.[11,12]

3.1.2.2 Aromatic ^1H chemical shifts

The ^1H chemical shifts belonging to the aromatic protons behaved as expected for fluorine-substituted aromatic rings.[27] Notably, the ^1H chemical shift assigned to proton(s) *ortho-* to the fluorine substitution were shifted upfield relative to the corresponding ^1H chemical shifts in DPPy for all six fluorine-substituted isomers. For example, in fluorolintane, the ^1H shift assigned to $H_{3'}$ was shifted ~0.25 ppm upfield relative to the corresponding $H_{3'}$ shift of DPPy. A comparable effect was seen with respect to protons on the position of the ring *para-* to fluorine. For example, in the case of 3-F-DPPy, the assigned $H_{6'}$ was 0.25 ppm upfield relative to the corresponding shift in DPPy. The upfield shifts were attributed to the resonance donating effects of fluorine.[27] As expected, the ^1H chemical shifts assigned to protons

meta- to the fluorine substitution were shifted downfield relative to DPPy for all six isomers, though in some cases the effect was only modest. For example, the ^{1}H chemical shift for 4-F-DPPy assigned to $H_{2',6'}$ (*meta* to 4-F) was 0.1 ppm downfield relative to DPPy. In addition, the different *meta*-protons on the same compound were affected to a different extent, as can be seen with fluorolintane, where a shift of 0.6 ppm was observed for $H_{6'}$ but there was no comparable effect on $H_{4'}$ (relative to corresponding shifts in DPPy).This difference may be due to additional effects from the alkyl substitution on the ring. The corresponding downfield shifts for protons attached to carbons *meta*- to the fluorine substituted carbon were consistent with the inductive withdrawing effect of fluorine that is most apparent on the relative meta-positions of the aromatic ring, which do not experience resonance donating effects.[27]

3.1.2.3 ^{13}C chemical shifts

The ^{13}C chemical shift assignments for DPPy, fluorolintane and its 5 positional isomers are presented in <mark>Table 3</mark> and refer to the hydrochloride salts. The C_1 ^{13}C chemical shift for 2-F-DPPy was ~8 and ~7 ppm upfield relative to the corresponding shift of DPPy and 3-F- and 4-F-DPPy isomers respectively. Interestingly, a similar upfield shift for C_2 was observed for 2''-F-DPPy of ~7 and 6 ppm for DPPy and 3''-F- and 4''-F-DPPy isomers, respectively. As stated previously, C_α and C_β each gave two ^{13}C chemical shifts, which correlated to two protons each in the HMQC spectra.

Fluorine substitution led to a large downfield shift relative to DPPy for all fluorine isomers, with the *ipso*-carbon shifts appearing around 160 ppm. [13]C shifts assigned to carbons *ortho*- to the CF carbon were shifted upfield relative to the corresponding shift in DPPy. For example, for fluorolintane, $C_{1'}$ and $C_{3'}$ shifts were shifted ~12.5 ppm upfield relative to DPPy and similar shifts were seen for the other five isomers. In the case of carbons *meta*- to fluorine, there was a slight downfield shift (~3 ppm). *Para*- [13]C chemical shifts exhibited an upfield shift (~3 ppm) relative to DPPy. Again, the upfield shifts seen with *ortho*- and *para*-positons relative to the CF carbon were expected and consistent with the resonance-donating effects of fluorine. Likewise, the downfield shift seen with carbons *meta*- to the fluorine substation were consistent with the inductive withdrawing effect of fluorine.[27] As described above, a comparable effect was observed in the corresponding ^{1}H spectra. HMBC was particularly helpful in distinguishing benzyl and phenyl fluorine series due to the expected correlations occurring between the C_1 positions ($C_{1'}$ and $C_{1''}$) of the aromatic rings and the C_1 and C_2 ethyl chain proton shifts.

3.1.2.4 Fluorine splitting of ^{13}C chemical shifts and ^{19}F NMR

Fluorine substitution is known to split ^{13}C chemical shifts belonging to ipso- and adjacent carbons (3-4 bonds) due to coupling between ^{19}F-and ^{13}C nuclei. In the present experiments, these splits were observed for all six F-DPPy isomers. The J-values were found to be greatest for C-ipso (246 Hz), ortho- to the CF carbon (0-~22.2 Hz), followed by meta- (~0-8.1 Hz) and lastly para- (0-3 Hz). These coupling constants were consistent with those expected based on studies with fluorobenzene and related compounds.[27] This feature can help with assignments of ^{13}C chemical shifts on fluorinated aromatic rings.[19]F chemical shifts for the six F-DPPy isomers is

presented in <mark>Table 4</mark>. Chemical shifts ranged from -111.58 to -117.10. The rank order from most downfield to most upfield was observed as follows: 3-F > 3''-F > 4-F > 4''-F > 2-F > 2''-F.

4. Conclusion

Fluorolintane (1-[1-(2-fluorophenyl)-2-phenylethyl]pyrrolidine, 2-F-DPPy) is a new psychoactive substance that belongs to the 1,2-diarylethylamine class and it appears that it might exert dissociative effects in humans. The presence of the fluorine substituent on either the phenyl and benzyl moieties gives rise to a total number of six possible racemic isomers, namely 2-F-, 3-F-, and 4-F-DPPy (phenyl) and 2''-F-, 3''-F-, and 4''-F-DPPy (benzyl), which adds to the analytical challenges that might be encountered in forensic investigations and/or toxicological casework. The isomers could be differentiated by NMR but subjecting the substances to chemical ionization triple quadrupole tandem mass spectrometric analysis was considered particularly useful when it transpired that the product ion mass spectra derived from the [M + H – HF]$^+$ species facilitated the differentiation between all six racemic isomers. GC-MS analyses were unable to result in complete differentiation whereas analysis by HPLC provided adequate separation between 2-F-, 3-F-, and 4-F-DPPy and 2''-F-, 3''-F-, and 4''-F-DPPy. The use of GC condensed phase IR was also employed successfully.
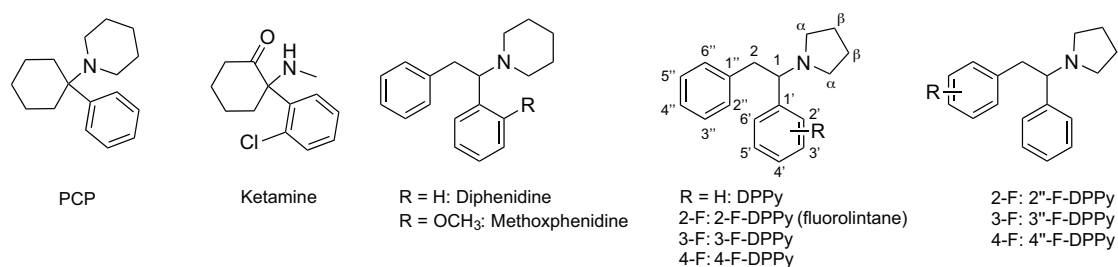
References

1. Tainter ML, Luduena FP, Lackey RW, Neuru EN. Actions of a series of diphenyl-ethylamines. *J Pharmacol Exp Ther.* 1943;77(4):317-323.
2. Dodds EC, Lawson W, Simpson SA, Williams PC. Testing diphenylethylamine compounds for analgesic action. *J Physiol.* 1945;104(1):47-51.
3. Heinzelman RV, Aspergren BD. Compounds containing the pyrrolidine ring. Analogs of sympathomimetic amines. *J Am Chem Soc.* 1953;75(14):3409-3413.
4. Palmer GC, Hutchison JB. Preclinical and clinical aspects of remacemide hydrochloride. In: Herrling PL, ed. *Excitatory Amino Acids. Clinical Results with Antagonists*. San Diego, CA, USA: Academic Press; 1997:109-120.
5. Machado-Vieira R, Henter ID, Zarate CA, Jr. New targets for rapid antidepressant action. *Prog Neurobiol.* 2017;152:21-37.
6. Morris H, Wallach J. From PCP to MXE: a comprehensive review of the non-medical use of dissociative drugs. *Drug Test Anal.* 2014;6(7-8):614-632.
7. Wallach J, Brandt SD. 1,2-Diarylethylamine- and ketamine-based new psychoactive substances. *Handb Exp Pharmacol.* 2019;252:305-352.
8. Wallach J, Brandt SD. Phencyclidine-based new psychoactive substances. *Handb Exp Pharmacol.* 2018;252:261-303.
9. Gray NM, Cheng BK. 1,2-Diarylethylamines for treatment of neurotoxic injury. Patent No. EP346791A1. G.D. Searle and Co. USA. 1989.
10. Wallach J, De Paoli G, Adejare A, Brandt SD. Preparation and analytical characterization of 1-(1-phenylcyclohexyl)piperidine (PCP) and 1-(1-

phenylcyclohexyl)pyrrolidine (PCPy) analogues. *Drug Test Anal.* 2014;6(7-8):633-650.

11. Wallach J, Kavanagh PV, McLaughlin G, et al. Preparation and characterization of the 'research chemical' diphenidine, its pyrrolidine analogue, and their 2,2-diphenylethyl isomers. *Drug Test Anal.* 2015;7(5):358-367.

12. McLaughlin G, Morris N, Kavanagh PV, et al. Test purchase, synthesis, and characterization of 2-methoxydiphenidine (MXP) and differentiation from its *meta-* and *para*-substituted isomers. *Drug Test Anal.* 2016;8(1):98-109.

13. Wallach J, Kang H, Colestock T, et al. Pharmacological investigations of the dissociative 'legal highs' diphenidine, methoxphenidine and analogues. *PloS one.* 2016;11(6):e0157021.

14. Kang H, Park P, Bortolotto ZA, et al. Ephenidine: a new psychoactive agent with ketamine-like NMDA receptor antagonist properties. *Neuropharmacology.* 2017;112(Pt A):144-149.

15. Colestock T, Wallach J, Mansi M, et al. Syntheses, analytical and pharmacological characterizations of the 'legal high' 4-[1-(3-methoxyphenyl)cyclohexyl]morpholine (3-MeO-PCMo) and analogues. *Drug Test Anal.* 2018;10(2):272-283.

16. National Slovenian Forensic Laboratory. National Slovenian Forensic Laboratory. Analytical report. Fluorolintane (C18H20FN). 1-(1-(2-fluorophenyl)-2-phenylethyl)pyrrolidine. https://www.policija.si/apps/nfl_response_web/0_Analytical_Reports_final/FL UOROLINTANE-ID-1420-15-report_final.pdf [Accessed 03 February 2018]

17. Xie L-G, Dixon DJ. Tertiary amine synthesis via reductive coupling of amides with Grignard reagents. *Chem Sci.* 2017;8(11):7492-7497.

18. Hou G-H, Xie J-H, Wang L-X, Zhou Q-L. Highly efficient Rh(I)-catalyzed asymmetric hydrogenation of enamines using monodente spiro phosphonite ligands. *J Am Chem Soc.* 2006;128(36):11774-11775.

19. Zhou Q, Hou G, Xie J, Wang L. Process for preparation of spiro phosphinates as chiral ligands for hydrogenation of enamines [Chinese]. CN1887893.

20. Heinzelmann RV, Aspergren BD. Compounds containing the pyrrolidine ring. Analogs of sympathomimetic amines. *J Am Chem Soc.* 1953;75:3409-3413.

21. Le Gall E, Haurena C, Sengmany S, Martens T, Troupel M. Three-component synthesis of α-branched amines under Barbier-like conditions. *J Org Chem.* 2009;74(20):7970-7973.

22. Geyer PM, Hulme MC, Irving JPB, et al. Guilty by dissociation–development of gas chromatography-mass spectrometry (GC-MS) and other rapid screening methods for the analysis of 13 diphenidine-derived new psychoactive substances (NPSs). *Anal Bioanal Chem.* 2016;408(29):8467-8481.

23. McKenzie C, Sutcliffe OB, Read KD, et al. Chemical synthesis, characterisation and in vitro and in vivo metabolism of the synthetic opioid MT-45 and its newly identified fluorinated analogue 2F-MT-45 with metabolite confirmation in urine samples from known drug users. *Forensic Toxicol.* 2018;36(2):359-374.

24. Westphal F, Rösner P, Junge T. Differentiation of regioisomeric ring-substituted fluorophenethylamines with product ion spectrometry. *Forensic Sci Int.* 2010;194(1-3):53-59.

25. Westphal F, Junge T. Ring positional differentiation of isomeric N-alkylated fluorocathinones by gas chromatography/tandem mass spectrometry. *Forensic Sci Int.* 2012;223(1-3):97-105.

26. Nakazono Y, Tsujikawa K, Kuwayama K, et al. Differentiation of regioisomeric fluoroamphetamine analogs by gas chromatography–mass spectrometry and liquid chromatography–tandem mass spectrometry. *Forensic Toxicol.* 2013;31(2):241-250.

27. Dolbier W. R. Jr. *Guide to Fluorine NMR for Organic Chemists.* Hoboken, New Jersey: Wiley; 2009.

Figures

PCP   Ketamine   R = H: Diphenidine   R = H: DPPy   2-F: 2''-F-DPPy
                               R = OCH₃: Methoxphenidine 2-F: 2-F-DPPy (fluorolintane)   3-F: 3''-F-DPPy
                                                          3-F: 3-F-DPPy   4-F: 4''-F-DPPy
                                                          4-F: 4-F-DPPy

Figure 1. 1,2-Diarylethylamines and related arylcyclohexylamines including phencyclidine (PCP) and ketamine. The numbering scheme is used for NMR assignments. The naming of fluorolintane isomers (2-F-, 3-F-, and 4-F-DPPy) was based on historical reasons where the first phenyl ring has been used without a prime designation in alignment with PCP-based compounds and the 1,2-diarylethylamines.
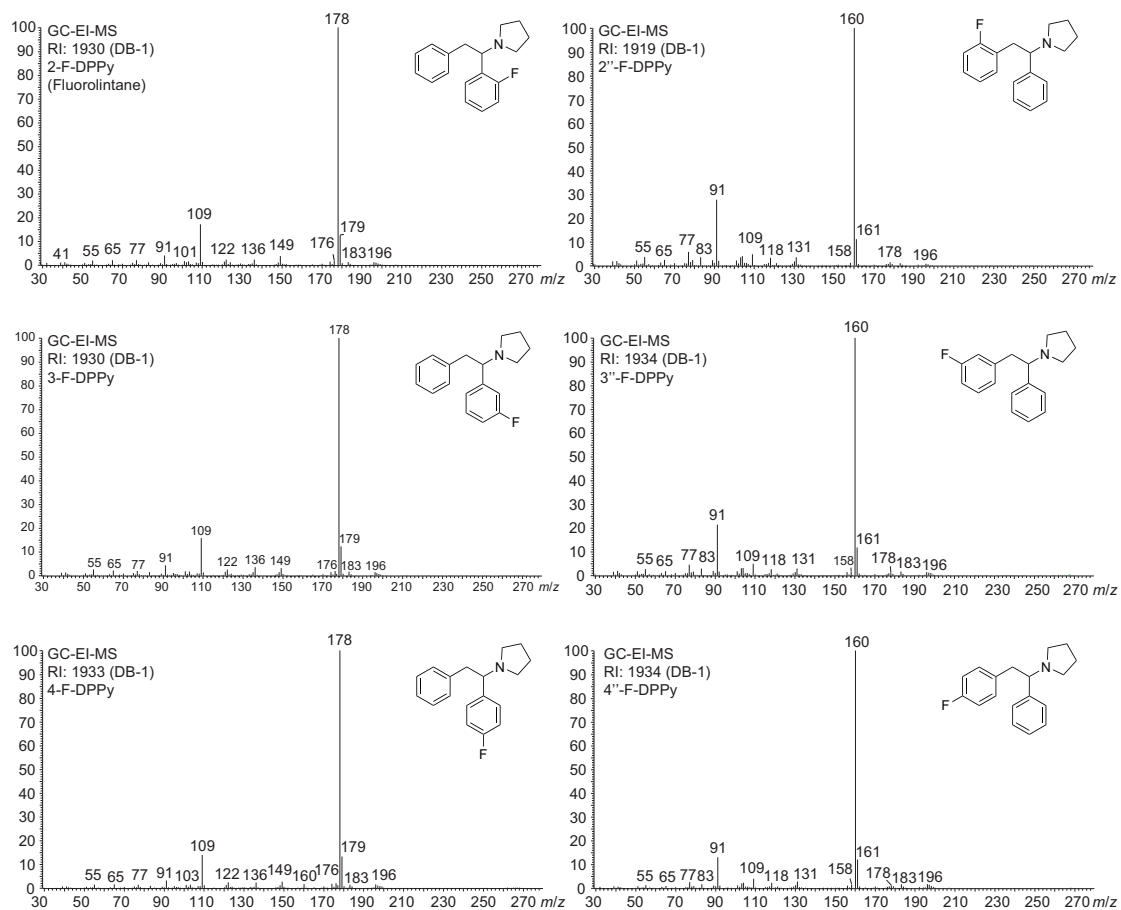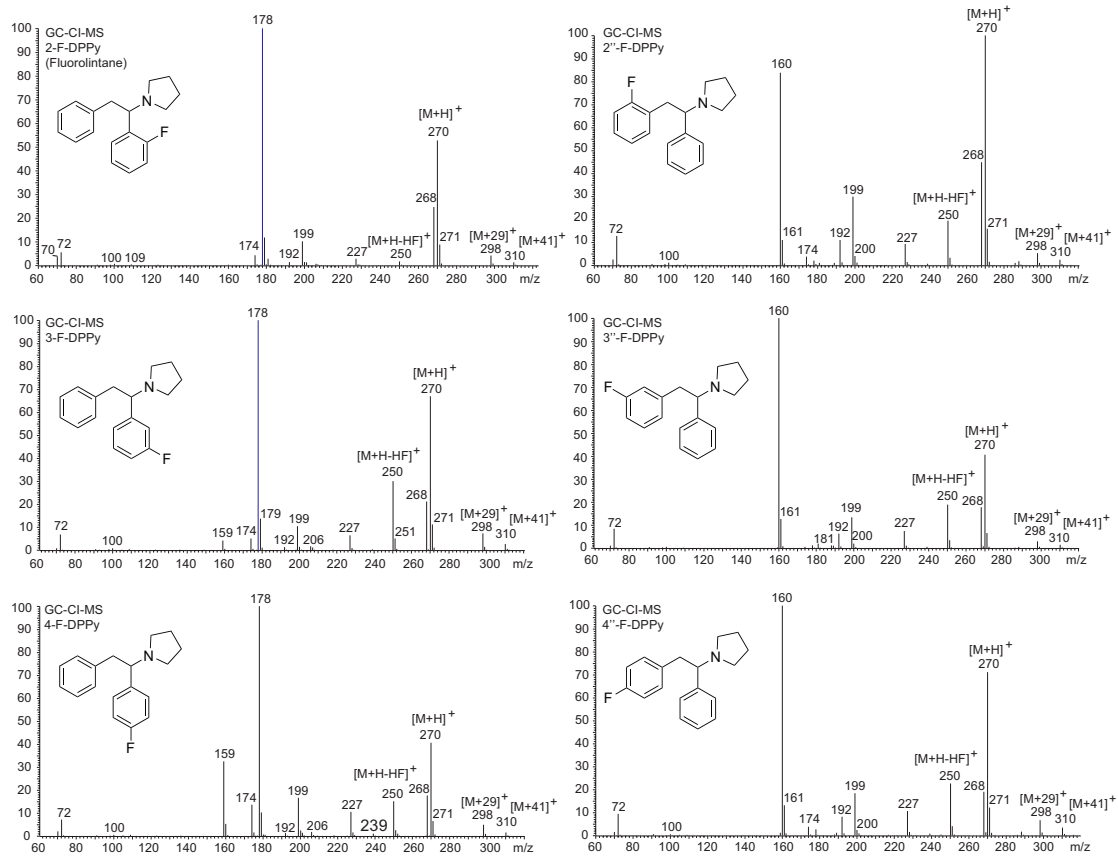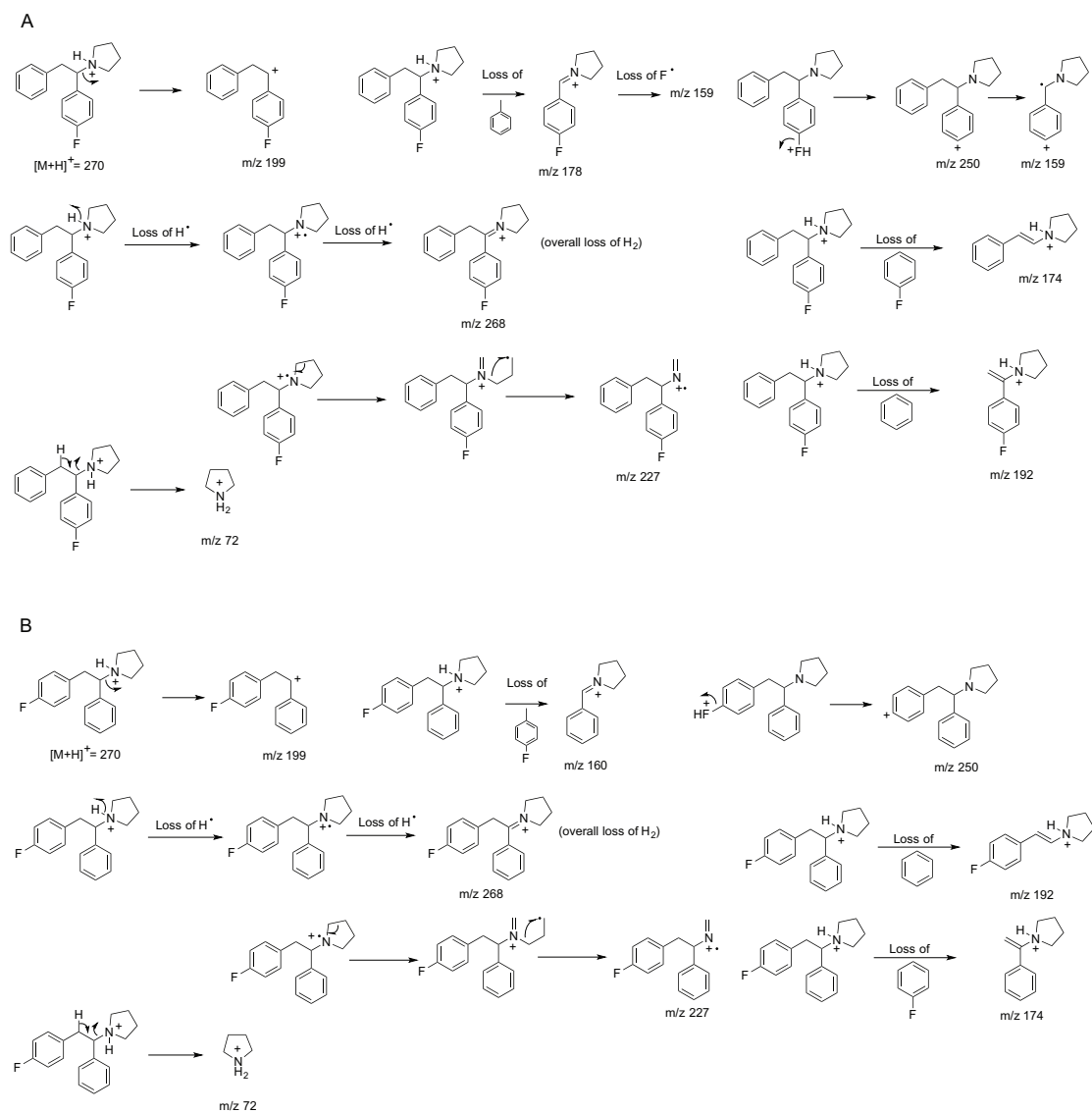
Figure 2. Electron ionization mass spectra of the two sets of three positional isomers.
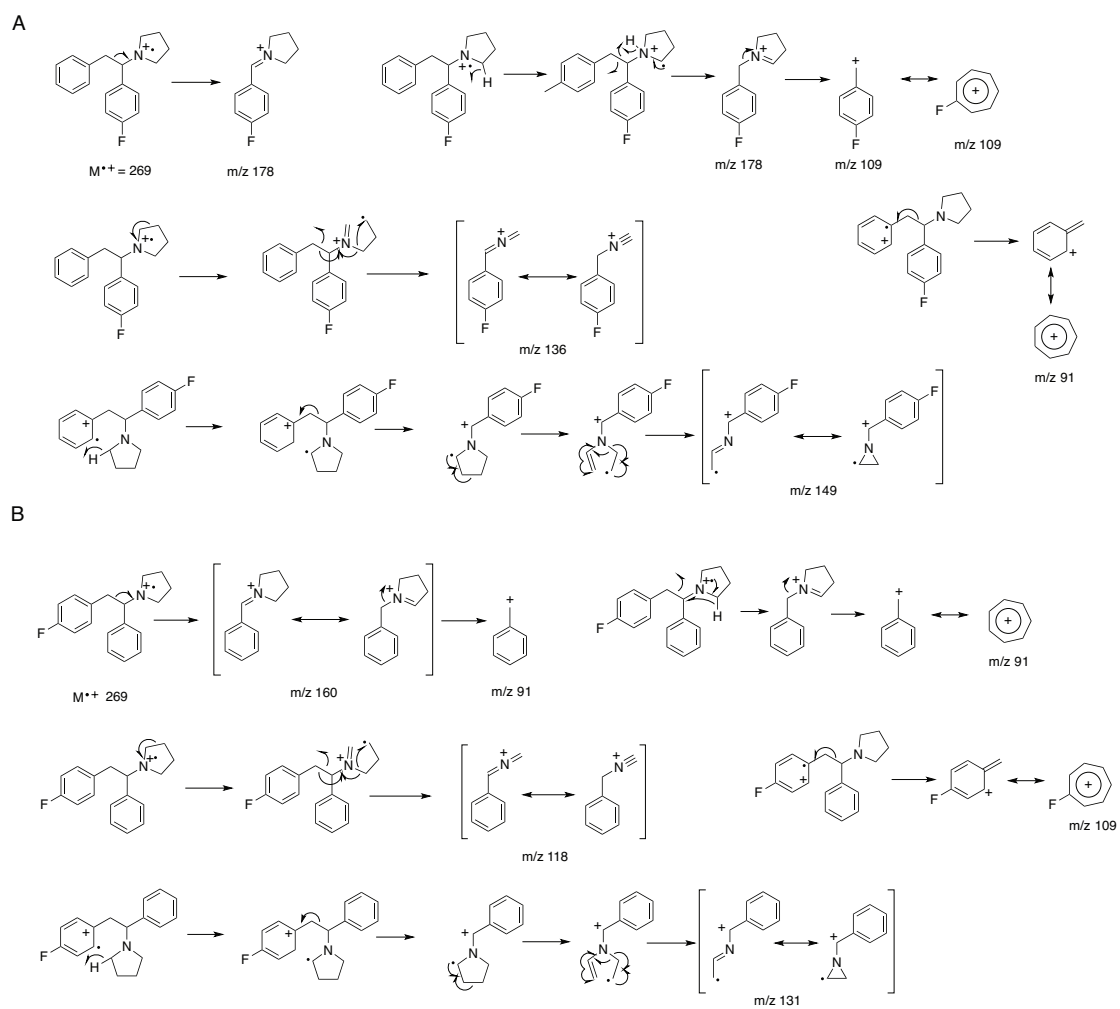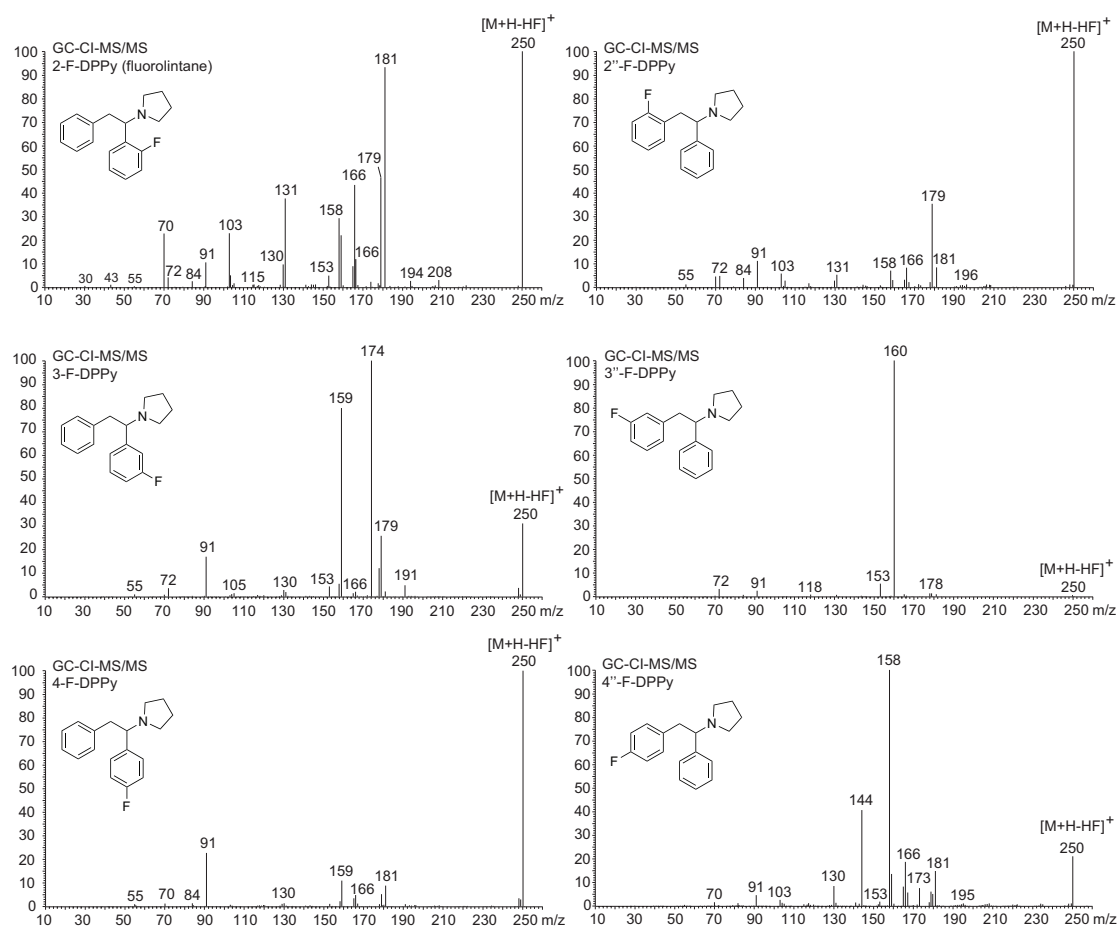
Figure 3. A. Proposed fragmentation pathways of 4-F-DPPy under electron ionization mass spectrometry conditions. B. Proposed fragmentation pathways of 4"-F-DPPy.
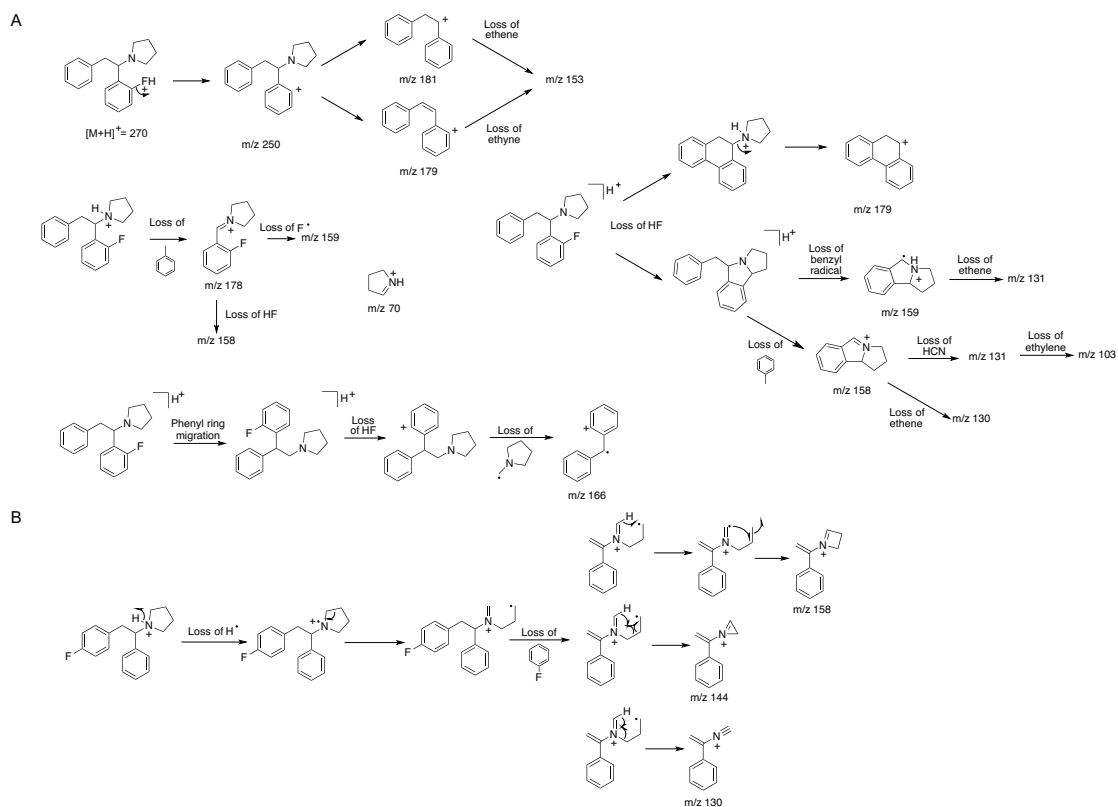
Figure 4. Gas chromatography chemical ionization mass spectra of the two sets of three positional isomers.
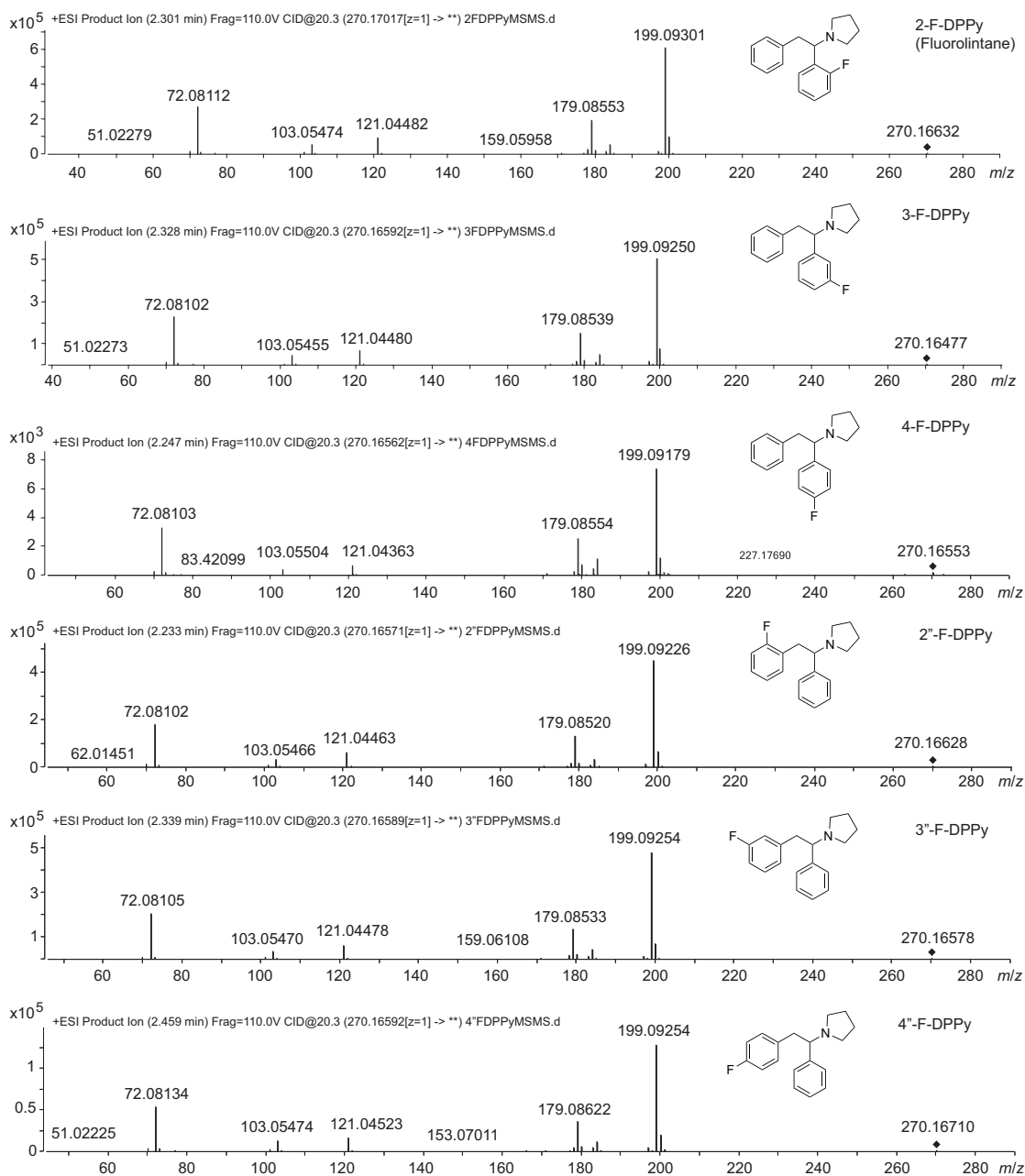
Figure 5. A. Proposed fragmentation pathways of 4-F-DPPy under chemical ionization tandem mass spectrometry conditions. B. Proposed fragmentation pathways of 4"-F-DPPy.

Figure 6. Gas chromatography product ion mass spectra of the [M + H − HF]$^+$ species that facilitated differentiation between all isomers.

Figure 7. Proposed chemical ionization tandem mass spectral fragmentation pathways originating from the [M + H – HF]$^+$ ion using 2-F-DPPy (fluorolintane) and 4''-F-DPPy as representative examples.
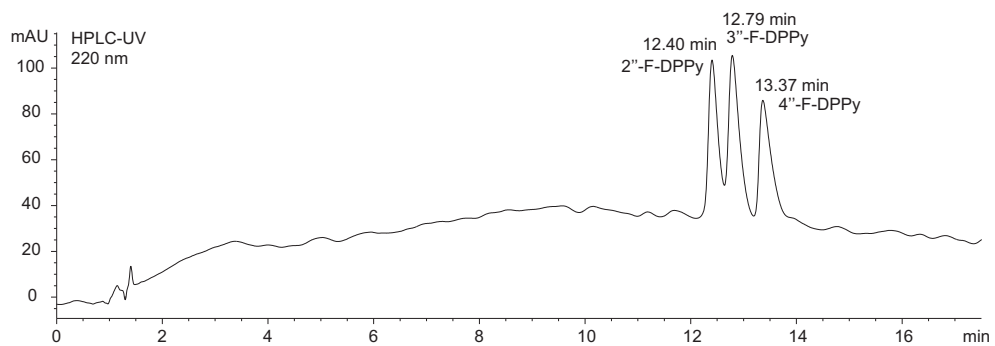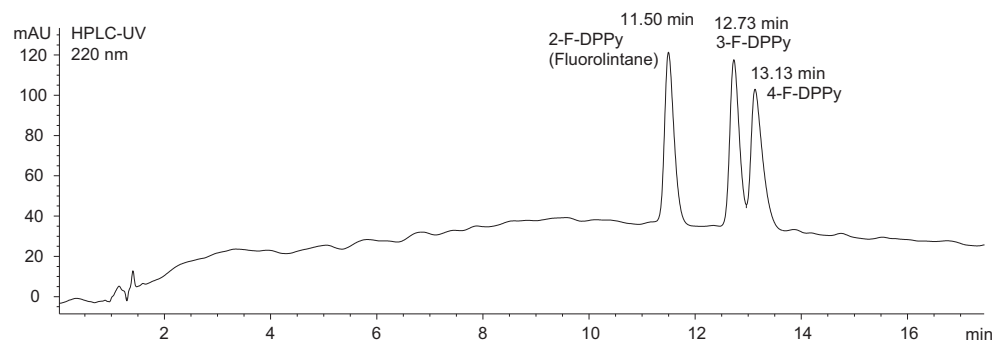
Figure 8. UHPLC-ESI-QTOF-MS/MS analysis results of the two sets of three positional isomers.
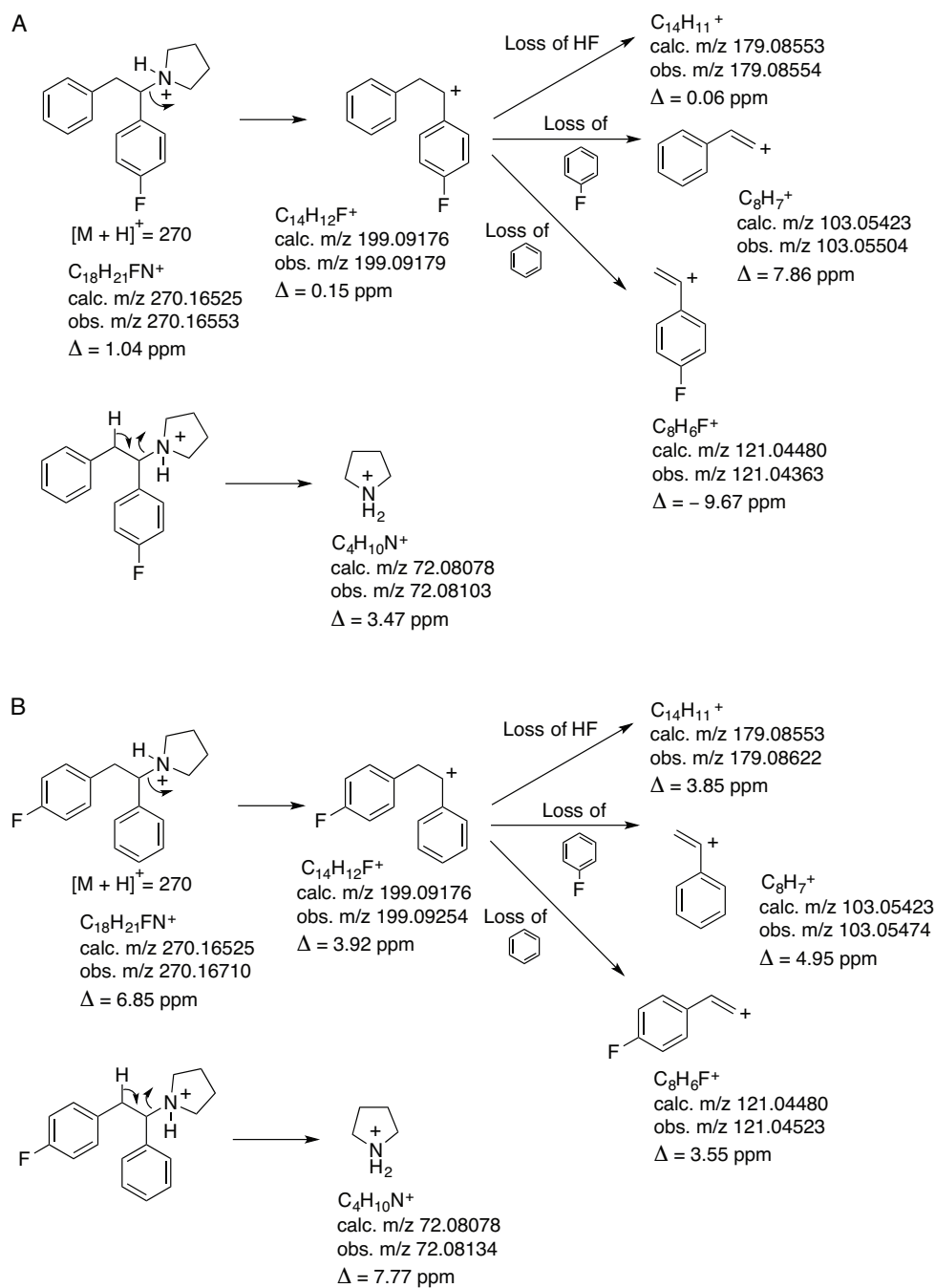
Figure 9. A. Proposed collision-induced dissociation pathways of 4-F-DPPy under quadrupole time-of-flight tandem mass spectrometry conditions. Proposed fragmentation pathways of 4"-F-DPPy.

Figure 10. High performance liquid chromatography ultraviolet analysis of all positional isomers using a Cosmosil πNAP column.
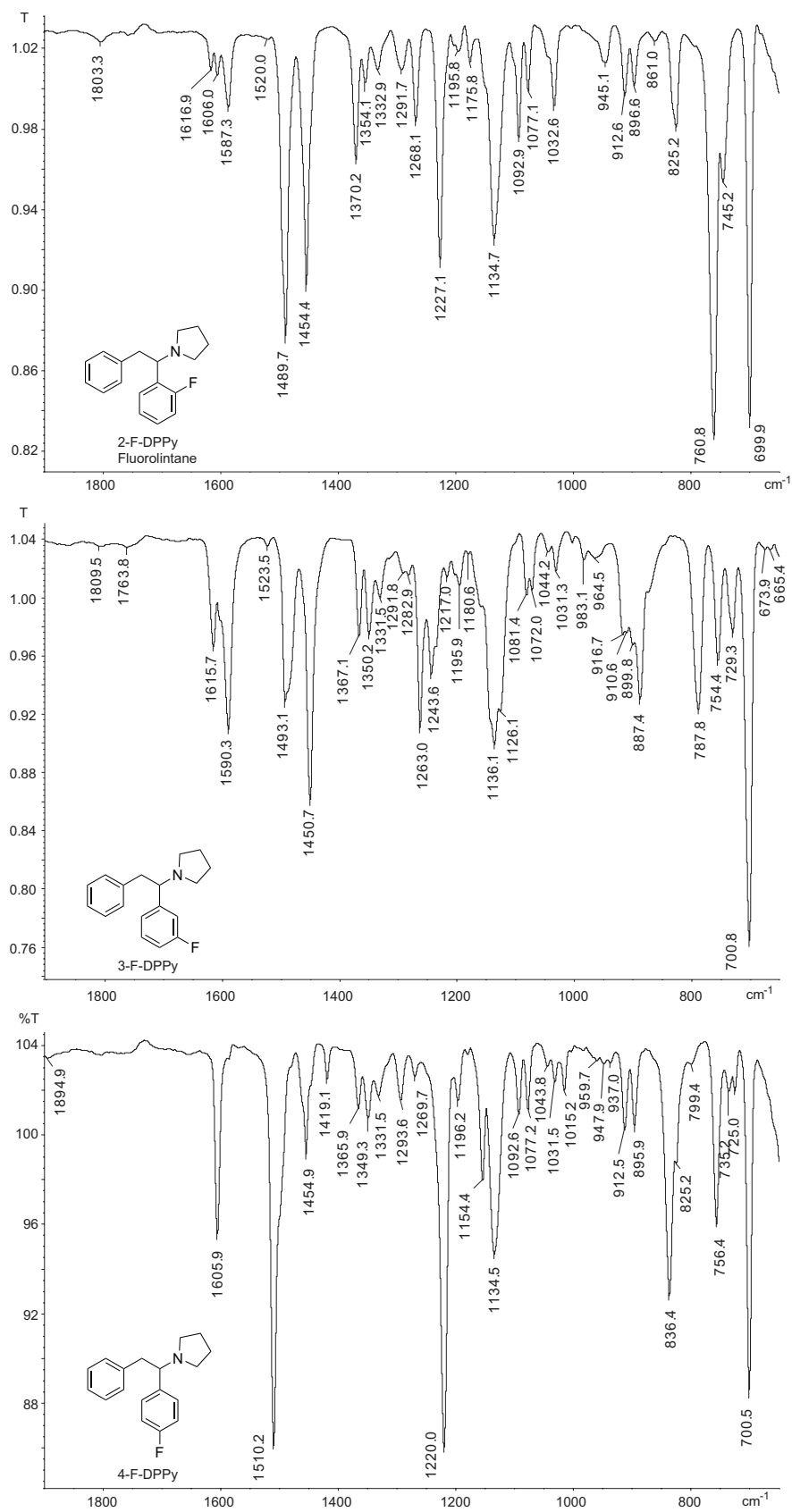
Figure 11. Gas chromatography condensed phase IR analysis of 2-F-, 3-F-, and 4-F-DPPy).

Figure 12. Gas chromatography condensed phase IR analysis of 2''-F-, 3''-F-, and 4''-F-DPPy).

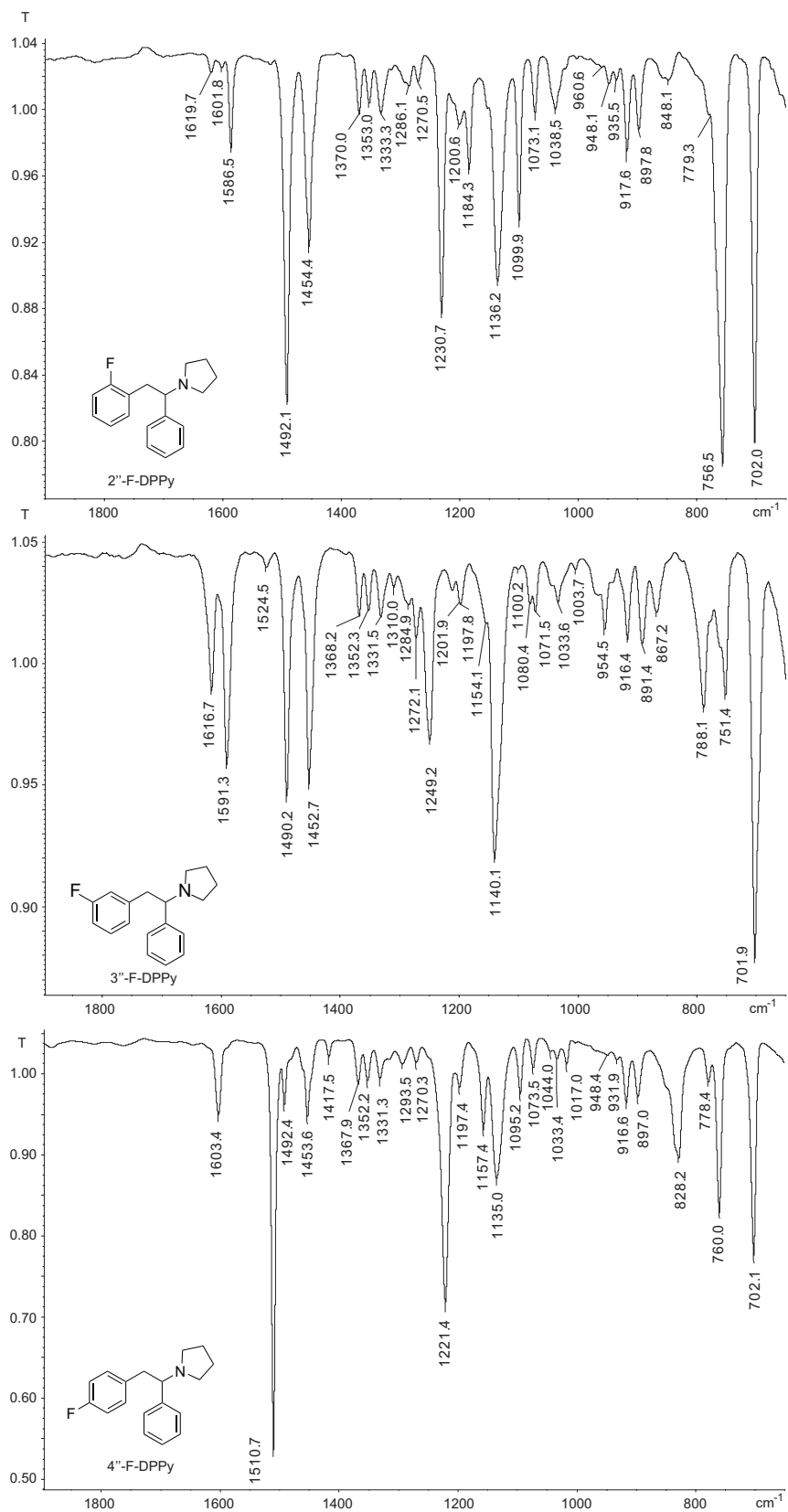**Table 1**. 400 MHz ^{1}H NMR of HCl salts. Twenty mg/mL in DMSO-d$_6$. Shifts in ppm and set to solvent reference (2.50 ppm).

^{1}H [δ / ppm]	DPPy	2-F-DPPy	3-F-DPPy	4-F-DPPy
H$_1$	4.60 (ddd, J = 12.1, 8.3, 4.1 Hz, 1H)	4.90 (ddd, J = 11.9, 8.1, 4.3 Hz, 1H)	4.65 (ddd, J = 11.9, 8.1, 4.2 Hz, 1H)	4.62 (ddd, J = 11.9, 8.5, 4.2 Hz, 1H)
H$_2$	3.62 (dd, J = 13.2, 4.1 Hz, 1H) 3.32 (t, J = 12.3 Hz, 1H) *overlap with H$_\alpha$	3.64 (dd, J = 13.0, 4.2 Hz, 1H) 3.30 (t, J = 12.4 Hz, 1H)	3.62 (dd, J = 13.2, 4.2 Hz, 1H) 3.34 – 3.21 (m, 1H) *overlap with H$_\alpha$	3.61 (dd, J = 13.2, 4.1 Hz, 1H) 3.28* (t, J = 12.5 Hz, 1H) *overlap with H$_\alpha$
H$_\alpha$	3.81 (ddd, J = 11.5, 6.6, 5.8 Hz, 1H) 3.37–3.25 (m 1H) *overlap with H$_2$ 2.94–2.85 (m, 1H) 2.83 (ddd, J = 15.5, 11.0, 8.5 Hz, 1H)	3.90-3.79 (m, 1H) 3.50–3.41 (m, 1H) 3.02 (s, 1H) 2.82–2.71 (ddd, J = 15.6, 8.4, 11.1 Hz, 1H)	3.88-3.77 (m, 1H) 3.34–3.21 (m, 1H) *Overlap with H$_2$ 3.0–2.90 (m, 1H) 2.90–2.77 (ddd, J = 15.5, 11.1, 8.3 Hz, 1H)	3.89-3.74 (m, 1H) 3.34–3.22 (m, 1H) *overlap with H$_2$ 2.99–2.86 (m, 1H) 2.86–2.72 (ddd, J = 15.5, 11.2, 8.5 Hz 1H)
H$_\beta$	2.10–1.92 (m, 2H) 1.92–1.74 (m, 2H)	2.10–1.79 (m, 4H)	2.09–1.95 (m, 2H) 1.95–1.87 (m, 1H) 1.86–1.74 (m, 1H)	2.00 (q, J = 8.2, 7.5 Hz, 2H) 1.90 (d, J = 8.9 Hz, 1H) 1.85–1.72 (m, 1H)
H$_{2'}$	7.65–7.47 (m, 2H)	–	7.51 (dm, J = 10.2 Hz, 1H)	7.70–7.49 (m, 1H)
H$_{3'}$	7.40–7.25 (m, 2H) *overlap with H$_{4'}$	7.12–7.03 (m, 1H) *overlap with H$_{4''}$	–	7.21–7.16 (m, 1H) *overlap with H$_{3'',5''}$
H$_{4'}$	7.40–7.25 (m, 1H) *overlap with H$_{3',5'}$	7.40–7.33 (m, 1H)	7.15–7.13 (m, 1H)	–
H$_{5'}$	7.40–7.25 (m, 2H) *overlap with H$_{4'}$	7.29 (td, J = 7.5, 1.3 Hz, 1H)	7.35 (td, J = 7.9, 5.9 Hz, 1H)	7.21–7.16 (m, 1H) *overlap with H$_{3'',5''}$
H$_{6'}$	7.65–7.47 (m, 2H)	8.14 (t, J = 7.4 Hz, 1H)	7.30 (dt, J = 7.7, 1.4 Hz, 1H)	7.70–7.49 (m, 1H)
H$_{2''}$	6.98 (dm, J = 8.3 Hz, 2H)	7.03–6.97 (m, 1H),	7.04–6.97 (m, 1H)	6.99 (dm, J = 8.3 Hz, 1H)

H$_{3''}$	7.12 (dm, J = 7.4 Hz, 2H)*overlap with H$_{4''}$	7.18–7.12 (m, 1H)	7.20–7.15 (m, 1H)	7.14 (dm, J = 7.4 Hz, 1H) *overlap with H$_{3',5'}$ and H$_{4''}$
H$_{4''}$	7.19–7.03 (dm, 1H) *overlap with H$_{3'',5''}$	7.12–7.03 (m, 1H) *overlap with H$_{3'}$	7.13–7.07 (m, 1H)	7.11–7.08 (m, 1H) *overlap with H$_{3'',5''}$
H$_{5''}$	7.12 (dm, J = 7.4 Hz, 2H) *overlap with H$_{4''}$	7.18–7.12 (m, 1H)	7.20–7.15 (m, 1H)	7.14 (dm, J = 7.4 Hz, 1H) *overlap with H$_{3',5'}$ and H$_{4''}$
H$_{6''}$	6.98 (dm, J = 6.9 Hz, 2H)	7.03–6.97 (m, 1H),	7.04–6.97 (m, 1H)	6.99 (dm, J = 8.3 Hz, 1H)
NH$^+$	11.98 (s, 1H)	11.82 (s, 1H)	11.84 (s, 1H)	11.74 (s, 1H)

Table 2. 400 MHz ^{1}H NMR of HCl salts. Twenty mg/mL in DMSO-d$_6$. Shifts in ppm set to solvent reference (2.50 ppm).

^{1}H [δ / ppm]	2''-F-DPPy	3''-F-DPPy	4''-F-DPPy
H$_1$	4.58 (ddd, J = 12.3, 8.6, 4.3 Hz, 1H)	4.61 (ddd, J = 12.1, 8.2, 4.1 Hz, 1H)	4.56 (ddd, J = 11.8, 7.7, 3.9 Hz, 1H)
H$_2$	3.59 (dd, J = 13.4, 4.2 Hz, 1H) 3.43 (t, J = 12.6 Hz, 1H)	3.64 (dd, J = 13.2, 4.0 Hz, 1H) 3.36–3.27 (m, 1H) *Overlap with H$_\alpha$	3.60 (dd, J = 13.2, 4.1 Hz, 1H) 3.34–3.24 (m, 1H) *Overlap with H$_\alpha$
H$_\alpha$	3.98–3.80 (m, 1H) 3.33–3.18 (m, 1H) 2.96–2.72 (m, 2H)	3.85–3.75 (m, 1H) 3.36–3.27 (m, 1H) *Overlap with H$_2$ 2.90–2.85 (m, 1H) 2.79 (dq, J = 10.0, 8.3 Hz, 1H)	3.85–3.76 (m, 1H) 3.34–3.24 (m, 1H *Overlap with H$_2$ 2.93–2.85 (m, 1H) 2.79 (dq, J = 10.2, 8.4 Hz, 1H)
H$_\beta$	2.08–1.95 (m, 2H) 1.95–1.85 (m, 1H) 1.85–1.73 (m, 1H)	2.06–1.95 (m, 2H) 1.94–1.86 (m, 1H) 1.86–1.73 (m, 1H)	2.10–1.95 (m, 2H) 1.94–1.85 (m, 1H) 1.86–1.75 (m, 1H)
H$_{2'}$	7.54 (dd, J = 6.7, 2.9 Hz, 2H)	7.57–7.50 (m, 2H)	7.53–7.50 (m, 2H)
H$_{3'}$	7.36–7.25 (m, 2H) *overlap with H$_{4'}$	7.37–7.28 (m, 2H) *overlap with H4''	7.36–7.28 (m, 2H) *overlap with H$_{4''}$

H$_{4'}$	7.36–7.25 (m, 1H) *overlap with H$_{3',5'}$	7.37–7.28 (m, 1H) *overlap with H$_{3,5''}$	7.36–7.28 (m, 1H) *overlap with H$_{3,5''}$
H$_{5'}$	7.36–7.25 (m, 2H) *overlap with H$_{4'}$	7.37–7.28 (m, 2H) *overlap with H$_{4''}$	7.36–7.28 (m, 2H)
H$_{6'}$	7.54 (dd, J = 6.7, 2.9 Hz, 2H)	7.57–7.50 (m, 2H)	7.53–7.50 (m, 2H)
H$_{2''}$	–	6.95–6.86 (m, 1H) *Overlap with H$_{4''}$	7.02–7.00 (m, 2H)
H$_{3''}$	7.08–7.0 (m, 1H) *overlap with H$_{6''}$	–	6.97–6.95 (m, 2H)
H$_{4''}$	7.20–7.11 (m, 1H)	6.95–6.86 (m, 1H) *overlap with H$_{2''}$	–
H$_{5''}$	6.96 (td, J = 7.6, 1.1 Hz, 1H)	7.16 (td, J = 7.9, 6.2 Hz, 1H)	6.97–6.95 (m, 2H)
H$_{6''}$	7.07–7.0 (m, 1H) *overlap with H$_{3''}$	6.80 (dt, J = 7.7, 1.2 Hz, 1H)	7.02–7.00 (m, 2H)
NH^{+}	11.90 (s, 1H)	11.67 (s, 1H)	11.72 (s, 1H)

Table 3. 101 MHz ^{13}C NMR of HCl salts. Twenty mg/mL in DMSO-d$_6$. Shifts in ppm, and set to solvent reference (39.52 ppm).

^{13}C [δ / ppm]	DPPy (pendant)	2-F-DPPy (pendant)	3-F-DPPy (pendant)	4-F-DPPy (^{13}C)	2''-F-DPPy (pendant)	3''-F-DPPy (pendant)	4''-F-DPPy (pendant)
C$_1$	69.67	61.73	68.97	68.76	68.56	69.28	69.68
C$_2$	38.08	37.55	38.00	38.06	31.49	37.65	37.21
C$_\alpha$	52.49 52.32	52.62 52.52	52.59 52.50	52.49 52.33	52.69 52.59	52.54 52.49	52.53 52.45
C$_\beta$	22.94 22.64	22.93 22.63	22.96 22.69	22.96 22.65	22.98 22.60	22.98 22.71	22.98 22.68
C$_{1'}$	135.05	121.93 121.79	137.83 137.76	131.35	134.84	134.79	134.90
C$_{2'}$	129.06	161.30 158.86	115.87 115.65 *overlap with H$_{4'}$	131.40 131.32	128.80	129.05	129.04
C$_{3'}$	128.60	115.59	163.14	115.65	128.61	128.74	128.70

		115.37	160.71	115.44			
C$_{4'}$	128.96	131.35 131.27	116.08 115.87 *overlap with H$_{2'}$	163.36 160.91	129.11	129.15	129.06
C$_{5'}$	128.60	125.07 125.04	130.74 130.66	115.65 115.44	128.61	128.74	128.70
C$_{6'}$	129.06	129.88	125.49 125.47	131.40 131.32	128.80	129.05	129.04
C$_{1''}$	136.14	135.45	135.85	136.02	122.92 122.77	139.05 138.97	132.32 132.29
C$_{2''}$	129.16	129.09	129.17	129.18	161.52 159.09	116.04 115.83	131.11 131.03
C$_{3''}$	128.15	128.18	128.26	128.24	115.20 114.98	163.08 160.66	115.04 114.83
C$_{4''}$	126.47	126.71	126.62	126.56	128.95 128.87	113.52 113.31	162.06 159.65
C$_{5''}$	128.15	128.18	128.26	128.24	124.22 124.19	130.11 130.03	115.04 114.83
C$_{6''}$	129.16	129.09	129.17	129.18	131.58 131.53	125.46 125.43	131.11 131.03

Table 4. 376.5 MHz ^{19}F NMR of HCl salts. Twenty mg/mL in DMSO-d$_6$. Reference CFCl$_3$ (0.00 ppm).

Compound	^{19}F NMR
2-F-DPPy	-116.29
3-F-DPPy	-111.58
4-F-DPPy	-112.05
2''-F-DPPy	-117.10
3''-F-DPPy	-113.08
4''-F-DPPy	-115.79